ACS central science

Research Article

http://pubs.acs.org/journal/acscii

Record Atmospheric Fresh Water Capture and Heat Transfer with a Material Operating at the Water Uptake Reversibility Limit

Adam J. Rieth,[†] Sungwoo Yang,[‡] Evelyn N. Wang,[‡] and Mircea Dincă*[,†]

[†]Department of Chemistry, Massachusetts Institute of Technology, 77 Massachusetts Avenue, Cambridge, Massachusetts 02139, United States

[‡]Department of Mechanical Engineering, Massachusetts Institute of Technology, 77 Massachusetts Avenue, Cambridge, Massachusetts 02139, United States

Supporting Information

ABSTRACT: The capture of water vapor at low relative humidity is desirable for producing potable water in desert regions and for heat transfer and storage. Here, we report a mesoporous metal−organic framework that captures 82% water by weight below 30% relative humidity. Under simulated desert conditions, the sorbent would deliver 0.82 g_{H2O} g_{MOF}^{-1}, nearly double the quantity of fresh water compared to the previous best material. The material further demonstrates a cooling capacity of 400 kWh m^{-3} per cycle, also a record value for a sorbent capable of creating a 20 °C difference between ambient and output temperature. The water uptake in this sorbent is optimized: the pore diameter of our material is above the critical diameter for water capillary action, enabling water uptake at the limit of reversibility.

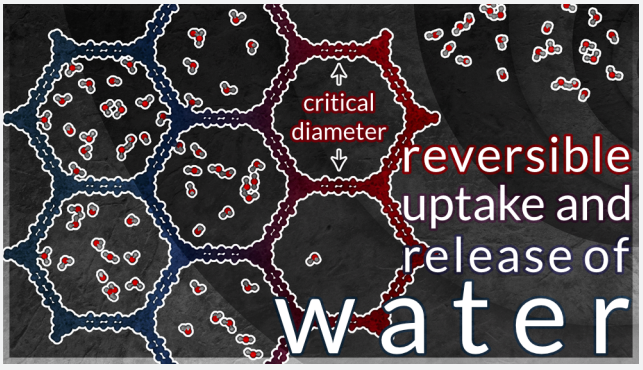

Fresh water necessities are projected to increase at an even faster pace than demands for energy, itself facing a severe shortfall in the next decades.[1,2] The projected water shortfall for 2030 is almost 2000 billion m^3, more than 20% of the projected global needs.[3] Our planet does not lack water, it is just either too salty or locked in ice. Whereas desalination produces relatively cheap fresh water, it requires a distribution infrastructure and large upfront capital cost.[4,5] An important challenge for water production is the distributed capture of water from the atmosphere, generating water locally where it is currently scarce or contaminated.[6] Current atmospheric water generators (AWGs) function either by chilling air below its dew point or by distilling water absorbed in concentrated brine, both of which require large energy input.[7] Solid sorbents that use natural variations between daytime and nighttime temperature and relative humidity (RH) to capture and release water are an alternative that requires no additional energy input.[8]

Sorbents with large capacity for water uptake can also address energy and environmental challenges related to heat transfer[9] by implementation in adsorption heat pumps (AHPs).[10−14] These create temperature gradients for heating or cooling by using waste heat resources, such as engine exhaust, and a working fluid with a high enthalpy of evaporation, such as water (40.7 kJ mol^{-1}).[10] In light of the recent agreement to phase out hydrofluorocarbons,[15] AHPs are an attractive alternative, but their miniaturization and wide deployment are limited by the low water capacity of the active sorbents currently employed.[10] Here, we report that a mesoporous metal−organic framework (MOF) exhibits water absorption behavior and total uptake that address critical challenges in both fresh water capture and heat pump applications.

In choosing the optimal water sorbent, stability, hydrophilicity, and pore diameter are of critical importance. MOFs offer the flexibility required to optimize all these parameters at once, an otherwise difficult task for a single material. Because water stability can be a challenge for such materials, early transition metal carboxylates[16,17] and metal azolates[18,19] that are extremely stable to water represent logical choices for water sorption. The pore hydrophilicity must be sufficient to allow for water nucleation and pore filling below approximately 30% RH for most applications.[10,13] Finally, to avoid undesirable hysteresis upon water desorption, the pore size must be below the critical diameter (D_c) of the working fluid, defined as the pore size at which the mechanism for adsorption changes from continuous pore filling to hysteretic capillary condensation.[20] For vapor phase liquids, D_c is given by the equation $D_c = 4\sigma T_C/(T_C - T)$, where σ and T_C are the van der Waals diameter and critical temperature of the adsorbate, respectively, and T is the adsorption temperature.[12,21] For water, D_c is 20.76 Å at 25 °C, implying that an adsorbent with a pore diameter of approximately 20 Å will maximize the internal volume available

Received: April 28, 2017
Published: May 24, 2017

DOI: 10.1021/acscentsci.7b00186
ACS Cent. Sci. 2017, 3, 668−672

for filling with water while avoiding irreversible capillary condensation.

One set of materials that satisfy all these parameters are the series $M_2Cl_2(BTDD)$ (M = Mn (**1**), Co (**2**), Ni (**3**); BTDD = bis(1*H*-1,2,3-triazolo[4,5-*b*],[4′,5′-*i*])dibenzo[1,4]dioxin) (Figure 1, Scheme S1).[22,23] These materials feature large mesoporous channels with a diameter of 22 Å, close to the D_c of water.

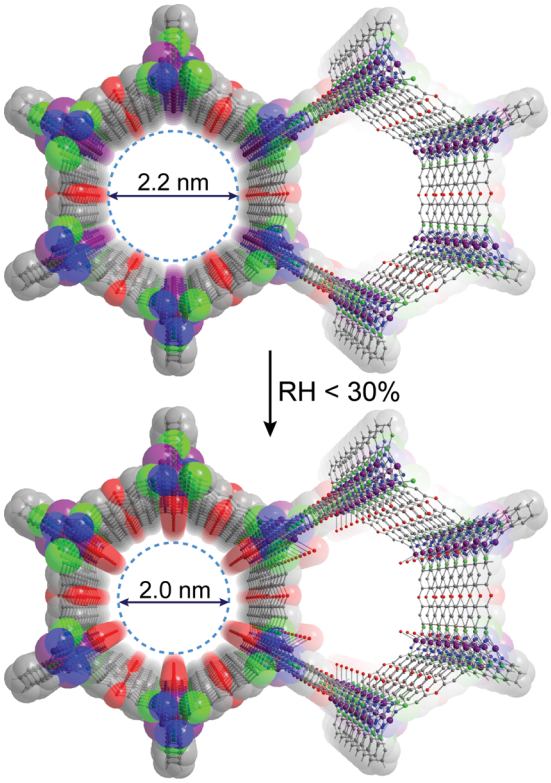

Figure 1. Structure of **2** projected along the *c* axis: Co, purple; C, gray; N, blue; O, red; Cl, green. Hydrogen atoms are omitted for clarity. At low RH, water is absorbed at the open coordination sites of the Co atoms, decreasing the pore diameter from slightly above to slightly below the D_c of water, enabling water uptake by reversible continuous pore filling.

The pores are defined by one-dimensional chains of five-coordinate metal atoms with hydrophilic open coordination sites supported by strong metal−azolate linkages. Because of all these attributes, the materials exhibit exceptional stability toward polar analytes such as ammonia,[22] and we anticipated that they would also have optimal water sorption properties. Water vapor adsorption isotherms were measured at 298 K for **1**, **2**, and **3** (Figure 2A). All materials show type IV isotherms featuring a step in the uptake at approximately 0.28 P/P_o (equivalent to RH = 28%), which is attributed to the onset of pore filling. Before this step, the water adsorbed is likely due to cluster adsorption around the open metal sites.[20] For **1**, the onset of pore filling is concurrent with pore collapse and structural rearrangement, as evidenced by the much lower total uptake of 0.389 g_{H2O} g_{MOF}^{-1}, a powder X-ray diffraction pattern consistent with largely amorphous material (Figure S1), and a greatly reduced apparent surface area (Figure S2). In contrast, **2** and **3** exhibit large and steep uptake steps as their pores are filled with water. These materials remain crystalline after water sorption and retain their high BET surface areas of 1912 m^2 g^{-1}

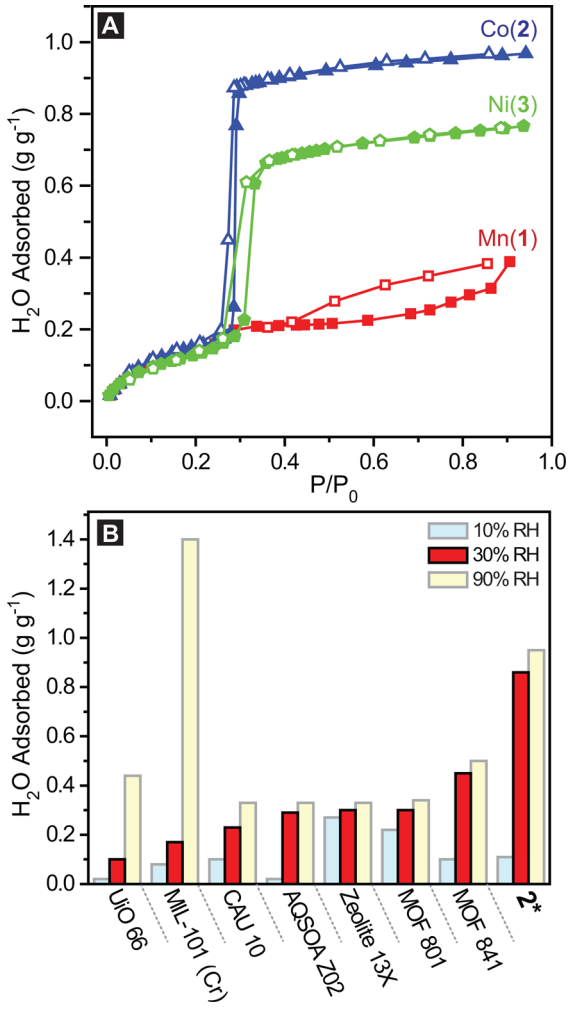

Figure 2. (A) Water vapor adsorption (closed symbols) and desorption (open symbols) at 298 K for **1** (red squares), **2** (blue triangles), and **3** (green pentagons). (B) Comparison of MOF and zeolites investigated for water sorption.[16,24,26] Materials that take up water between 10% and 30% RH are desirable for their strong affinity for water and their relative ease of regeneration. *This work.

and 1762 m^2 g^{-1}, respectively (Figures S3−S6). At 94% RH, the total water uptakes for **2** and **3** are 0.968 g g^{-1} and 0.766 g g^{-1}, respectively (Figure 2A). The lack of hysteresis between adsorption and desorption indicates continuous reversible pore filling rather than irreversible capillary condensation.[12] The uptake of water between 10% and 30% RH is referred to as the deliverable capacity because uptake in this region is due to a process with a high enough driving force to be useful in AWG and AHP applications, while allowing low-temperature regeneration.[24] Figure 2B illustrates the superiority of **2**, on a material basis in this humidity range, as compared to other MOFs and zeolites that have been investigated for their water uptake properties.[16,24−26]

Owing to its superior water adsorption behavior, Co_2Cl_2BTDD (**2**) was investigated in greater detail with respect to its potential utility in AWGs and AHPs. The heat of adsorption for water in **2**, determined by variable temperature water sorption isotherms fitted to the Clausius−Clapeyron equation, is approximately 55 kJ mol^{-1} at zero coverage and falls to 45.8 kJ mol^{-1} during pore filling (Figure S7). The latter is closer to the heat of vaporization for water, 40.7 kJ mol^{-1},

DOI: 10.1021/acscentsci.7b00186
ACS Cent. Sci. 2017, 3, 668−672

and indicates that water−water interactions are dominant during pore filling. The variable temperature water sorption isotherms also allow the calculation of a characteristic curve, which converts the independent pressure and temperature variables governing uptake into a single parameter related to the Gibbs free energy of adsorption (see the Supporting Information). In turn, the characteristic curve allows for the extrapolation of an isotherm at a given temperature to temperature and pressure values relevant for various devices.[10,27,28] The characteristic curve for **2** (Figure S8) was validated by measuring water vapor isotherms at 283, 293, and 298 K (Figure S9). We then used this characteristic curve to generate adsorption and desorption isotherms at temperatures relevant for AHP and AWG applications (Figures S10 and S11).

The potential of **2** to generate potable water in desert regions was evaluated by simulating realistic day/night temperature and RH conditions applicable in the Atacama,[29] the Sonoran,[30] and the Arabian[8] deserts, among others: daytime values of 45 °C and 5% RH changing to nighttime values of 25 °C and 35% RH.[8] Based on characteristic curve-derived isotherms under these conditions, **2** is predicted to capture 82% water by weight (wt %) at night and release it during the day (Figure 3A). This is nearly double the previous best material reported for this application, MOF-841, which captures and releases only 42 wt % water.[8] Cycling **2** under simulated desert daytime and nighttime conditions revealed an initial deliverable capacity of 84.7 wt %, in remarkable agreement with the characteristic curve predictions, a value that declined by only 5.1 wt % over 6 cycles (Figure 3B). Highlighting the exciting prospects of **2** for water capture is an elegant recent proof of principle study showing a device that delivers 0.30 L_{H2O} kg^{-1}_{MOF} per cycle using MOF-801 as the active adsorbent.[25] In a similar device, **2** is projected to capture and release 0.87 L_{H2O} kg^{-1}_{MOF} per cycle.

The thermodynamic parameters of water sorption in **2** highlight its exceptional performance at transferring heat. The water−**2** fluid−adsorbent working pair achieves a 20 °C temperature lift, the range required for an air conditioner, for instance.[10] This temperature difference can be achieved with a cooling capacity per cycle of ∼400 kWh m^{-3} (Figure 4A), at least 50 kWh m^{-3} higher than that of any known adsorbent,

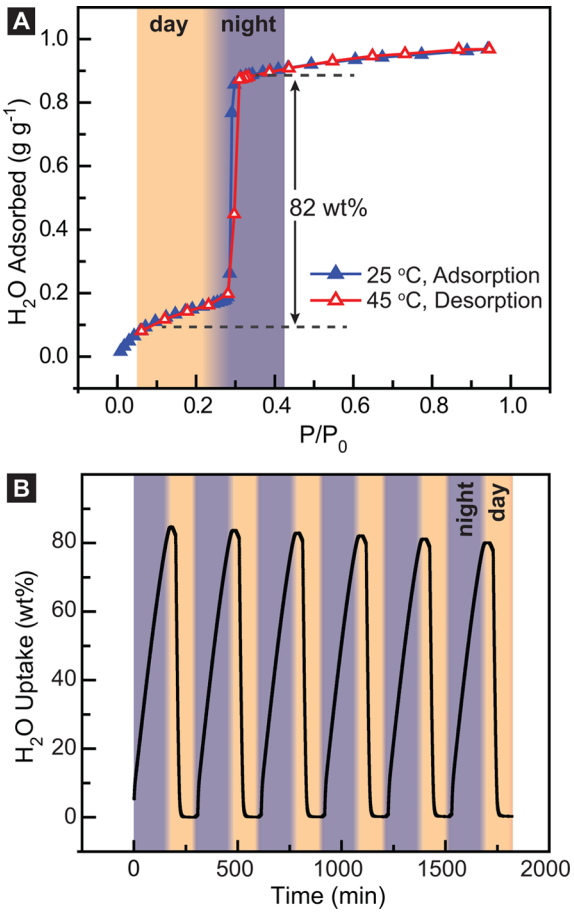

Figure 3. Performance of **2** in AWGs. (A) Estimation of the deliverable capacity of water from **2** under simulated desert conditions: daytime 45 °C and 5% RH and nighttime 25 °C and 35% RH. (B) Percent change in weight while cycling **2** between 45 °C and 5% RH (day), and 25 °C and 35% RH (night).

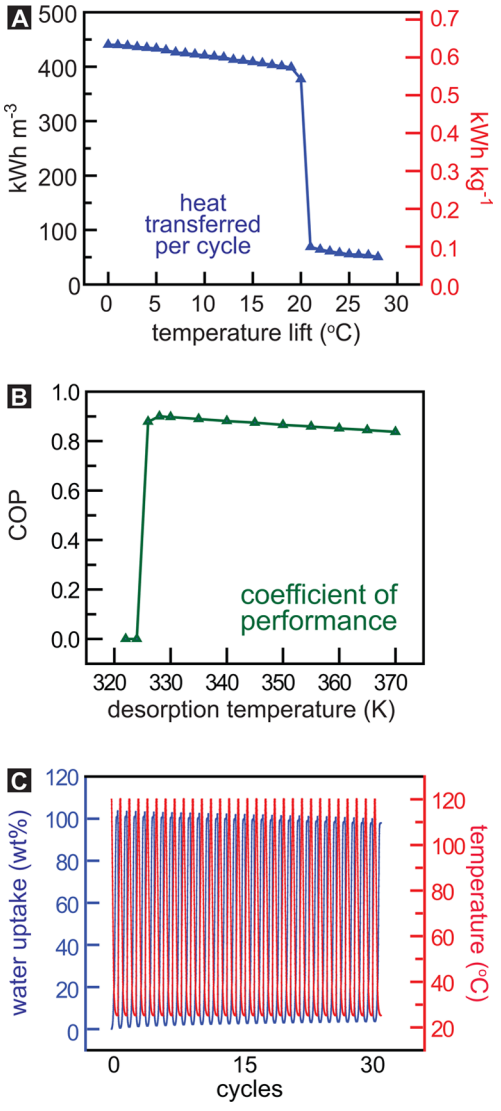

Figure 4. Performance of **2** in AHPs. (A) Volumetric (left axis) and gravimetric (right axis) heat energy transferred from ambient per cycle as a function of the temperature lift. (B) Material-based coefficient of performance for AHP cooling applications with a 20 °C temperature lift for the water−**2** working pair as a function of desorption temperature. (C) Temperature-swing water cycling of **2** at a constant water vapor pressure of 13 mmHg.

DOI: 10.1021/acscentsci.7b00186
ACS Cent. Sci. 2017, 3, 668−672

regardless of regeneration temperature.[10] In a hypothetical AHP using low-grade heat sources, compound **2** can be regenerated using waste heat of only 55 °C (Figure S12).[8,10] Such a device would have a material-based coefficient of performance (COP), defined as the ratio of useful cold energy output divided by input heat energy, of 0.885 (Figure 4B). A measure of efficiency, COPs for AHP cooling applications vary from 0 to 1. Notably, the water−**2** working pair has the highest COP for any fluid−adsorbent combination across a wide range of desorption temperatures.[10] The high COP for this material is a direct result of its unusually high gravimetric water capacity: very little energy is expended on heating the adsorbent because less solid is required for a given water capacity relative to other adsorbents. Compound **2** is stable to cycling under AHP conditions as well (Figure 4C). Cycling **2** between 25 and 120 °C at constant water vapor pressure of 13 mmHg revealed an initial gravimetric capacity greater than 1 g g^{-1}, with a decline of only 6.3 wt % and no loss in crystallinity after 30 cycles (Figure S5).

The data above position **2** as the best-known adsorbent for both AWGs and AHPs. With AHPs, reduction to practice is particularly attractive in vehicles, where combustion engines present a ready source of waste heat.[31] Practically, for an external temperature of 32 °C, the air conditioner output could be 12 °C using a regeneration temperature of only 55 °C. With AWGs, deployment of **2** in areas where temperature and RH swings between night and day straddle the adsorption step at 28% RH will allow distributed fresh water production, thus eliminating infrastructure needs. Although these particular sorbents have not been scaled up, recent work on the cost analysis of MOF production demonstrated that these materials can be produced economically at scale in a similar manner to other commodity chemicals.[32]

Fundamentally, these results demonstrate that adsorbents with pore sizes that match the critical diameter of a relevant working fluid should exhibit maximum uptake with limited hysteresis. The importance of the critical diameter is illustrated particularly well with Co_2Cl_2BTDD (**2**) here, whose open metal sites bind water prior to pore filling. This effectively reduces the pore diameter and makes it essentially equal to the critical diameter. Thereafter, water uptake accordingly proceeds by reversible continuous pore filling. Incorporation of uniformly distributed strongly adsorbing sites into materials with pore sizes larger than the critical diameter of the desired adsorbate should result in preadsorption prior to pore filling and should therefore serve as a general strategy for designing superior sorbents for both water capture and heat transfer applications.

■ ASSOCIATED CONTENT

Supporting Information

The Supporting Information is available free of charge on the ACS Publications website at DOI: 10.1021/acscentsci.7b00186.

Materials and methods, calculation methods, and Figures S1−S12 (PDF)

■ AUTHOR INFORMATION

Corresponding Author

*E-mail: mdinca@mit.edu.

ORCID

Mircea Dincă: 0000-0002-1262-1264

Notes

The authors declare the following competing financial interest(s): M.D., A.J.R., and MIT have filed a patent application pertaining to the results and materials presented here.

■ ACKNOWLEDGMENTS

This research was supported by the MIT Tata Center for Technology and Design. Fundamental studies of metal−small molecule interactions are supported by a National Science Foundation CAREER Award to M.D. (DMR-1452612). M.D. acknowledges the Sloan Foundation and the Research Corporation for Science Advancement (Cottrell Award) for nontenured faculty funds. S.Y. and E.N.W. acknowledge ARPA-E for partial support of this work. We thank Dr. C. H. Hendon for assistance with the production of the TOC graphic.

■ REFERENCES

(1) United Nations World Water Assessment Programme. *UN World Water Development Report: Managing Water under Uncertainty and Risk*, 4th ed.; 2012Vol. *1*, pp 1−407.

(2) Lewis, N. S.; Nocera, D. G. Powering the Planet: Chemical Challenges in Solar Energy Utilization. *Proc. Natl. Acad. Sci. U. S. A.* **2006**, *103* (43), 15729−15735.

(3) 2030 Water Resources Group. *Charting Our Water Future*; 2009.

(4) Shannon, M. A.; Bohn, P. W.; Elimelech, M.; Georgiadis, J. G.; Marinas, B. J.; Mayes, A. M. Science and Technology for Water Purification in the Coming Decades. *Nature* **2008**, *452*, 301−310.

(5) Elimelech, M.; Phillip, W. A. The Future of Seawater and the Environment: Energy, Technology, and the Environment. *Science* **2011**, *333*, 712−718.

(6) Water Abundance XPRIZE. water.xprize.org; 2016.

(7) Lee, A.; Moon, M. W.; Lim, H.; Kim, W. D.; Kim, H. Y. Water Harvest via Dewing. *Langmuir* **2012**, *28* (27), 10183−10191.

(8) Furukawa, H.; Gándara, F.; Zhang, Y.-B.; Jiang, J.; Queen, W. L.; Hudson, M. R.; Yaghi, O. M. Water Adsorption in Porous Metal-Organic Frameworks and Related Materials. *J. Am. Chem. Soc.* **2014**, *136* (11), 4369−4381.

(9) Shine, K. P.; Sturges, W. T. CO_2 Is Not the Only Gas. *Science* **2007**, *315*, 1804−1805.

(10) De Lange, M. F.; Verouden, K. J. F. M.; Vlugt, T. J. H.; Gascon, J.; Kapteijn, F. Adsorption-Driven Heat Pumps: The Potential of Metal-Organic Frameworks. *Chem. Rev.* **2015**, *115* (22), 12205−12250.

(11) Critoph, R. E. Evaluation of Alternative Refrigerant-Adsorbent Pairs for Refrigeration Cycles. *Appl. Therm. Eng.* **1996**, *16* (11), 891−900.

(12) Canivet, J.; Bonnefoy, J.; Daniel, C.; Legrand, A.; Coasne, B.; Farrusseng, D. Structure−property Relationships of Water Adsorption in Metal−organic Frameworks. *New J. Chem.* **2014**, *38* (7), 3102.

(13) Jeremias, F.; Lozan, V.; Henninger, S. K.; Janiak, C. Programming MOFs for Water Sorption: Amino-Functionalized MIL-125 and UiO-66 for Heat Transformation and Heat Storage Applications. *Dalton Trans.* **2013**, *42* (45), 15967−15973.

(14) Narayanan, S.; Yang, S.; Kim, H.; Wang, E. N. Optimization of Adsorption Processes for Climate Control and Thermal Energy Storage. *Int. J. Heat Mass Transfer* **2014**, *77*, 288−300.

(15) Greenblatt, J. B.; Wei, M. Assessment of the Climate Commitments and Additional Mitigation Policies of the United States. *Nat. Clim. Change* **2016**, *6*, 1090−1093.

(16) Akiyama, G.; Matsuda, R.; Sato, H.; Hori, A.; Takata, M.; Kitagawa, S. Effect of Functional Groups in MIL-101 on Water Sorption Behavior. *Microporous Mesoporous Mater.* **2012**, *157*, 89−93.

(17) Küsgens, P.; Rose, M.; Senkovska, I.; Fröde, H.; Henschel, A.; Siegle, S.; Kaskel, S. Characterization of Metal-Organic Frameworks by Water Adsorption. *Microporous Mesoporous Mater.* **2009**, *120* (3), 325−330.

DOI: 10.1021/acscentsci.7b00186
ACS Cent. Sci. 2017, 3, 668−672

(18) Choi, H. J.; Dincă, M.; Dailly, A.; Long, J. R. Hydrogen storage in Water-Stable Metal−organic Frameworks Incorporating 1,3- and 1,4-Benzenedipyrazolate. *Energy Environ. Sci.* **2010**, *3* (1), 117−123.
(19) Colombo, V.; Galli, S.; Choi, H. J.; Han, G. D.; Maspero, A.; Palmisano, G.; Masciocchi, N.; Long, J. R. High Thermal and Chemical Stability in Pyrazolate-Bridged Metal−organic Frameworks with Exposed Metal Sites. *Chem. Sci.* **2011**, *2* (7), 1311.
(20) Canivet, J.; Fateeva, A.; Guo, Y.; Coasne, B.; Farrusseng, D. Water Adsorption in MOFs: Fundamentals and Applications. *Chem. Soc. Rev.* **2014**, *43*, 5594−5617.
(21) Coasne, B.; Gubbins, K. E.; Pellenq, R. J. M. Temperature Effect on Adsorption/desorption Isotherms for a Simple Fluid Confined within Various Nanopores. *Adsorption* **2005**, *11*, 289−294.
(22) Rieth, A. J.; Tulchinsky, Y.; Dincă, M. High and Reversible Ammonia Uptake in Mesoporous Azolate Metal-Organic Frameworks with Open Mn, Co, and Ni Sites. *J. Am. Chem. Soc.* **2016**, *138* (30), 9401−9404.
(23) Tulchinsky, Y.; Hendon, C. H.; Lomachenko, K. A.; Borfecchia, E.; Melot, B. C.; Hudson, M. R.; Tarver, J. D.; Korzyński, M. D.; Stubbs, A. W.; Kagan, J. J.; Lamberti, C.; Brown, C. M.; Dincă, M. Reversible Capture and Release of Cl_2 and Br_2 with a Redox-Active Metal−Organic Framework. *J. Am. Chem. Soc.* **2017**, *139* (16), 5992−5997.
(24) Furukawa, H.; Gándara, F.; Zhang, Y.-B.; Jiang, J.; Queen, W. L.; Hudson, M. R.; Yaghi, O. M. Water Adsorption in Porous Metal-Organic Frameworks and Related Materials. *J. Am. Chem. Soc.* **2014**, *136* (11), 4369−4381.
(25) Kim, H.; Yang, S.; Rao, S. R.; Narayanan, S.; Kapustin, E. A.; Furukawa, H.; Umans, A. S.; Yaghi, O. M.; Wang, E. N. Water Harvesting from Air with Metal-Organic Frameworks Powered by Natural Sunlight. *Science* **2017**, *356*, 430.
(26) Goldsworthy, M. J. Measurements of Water Vapour Sorption Isotherms for RD Silica Gel, AQSOA-Z01, AQSOA-Z02, AQSOA-Z05 and CECA Zeolite 3A. *Microporous Mesoporous Mater.* **2014**, *196*, 59−67.
(27) De Lange, M. F.; Van Velzen, B. L.; Ottevanger, C. P.; Verouden, K. J. F. M.; Lin, L.-C.; Vlugt, T. J. H.; Gascon, J.; Kapteijn, F. Metal-Organic Frameworks in Adsorption-Driven Heat Pumps: The Potential of Alcohols as Working Fluids. *Langmuir* **2015**, *31* (46), 12783−12796.
(28) Cadiau, A.; Lee, J. S.; Damasceno Borges, D.; Fabry, P.; Devic, T.; Wharmby, M. T.; Martineau, C.; Foucher, D.; Taulelle, F.; Jun, C. H.; Hwang, Y. K.; Stock, N.; De Lange, M. F.; Kapteijn, F.; Gascon, J.; Maurin, G.; Chang, J. S.; Serre, C. Design of Hydrophilic Metal Organic Framework Water Adsorbents for Heat Reallocation. *Adv. Mater.* **2015**, *27* (32), 4775−4780.
(29) Cáceres, L.; Gómez-Silva, B.; Garró, X.; Rodríguez, V.; Monardes, V.; McKay, C. P. Relative Humidity Patterns and Fog Water Precipitation in the Atacama Desert and Biological Implications. *J. Geophys. Res. Biogeosci.* **2007**, *112* (4), 1−11.
(30) Unland, H. E.; Houser, P. R.; Shuttleworth, W. J.; Yang, Z.-L. Surface Flux Measurement and Modeling at a Semi-Arid Sonoran Desert Site. *Agric. For. Meteorol.* **1996**, *82* (1−4), 119−153.
(31) Narayanan, S.; Li, X.; Yang, S.; Kim, H.; Umans, A.; McKay, I. S.; Wang, E. N. Thermal Battery for Portable Climate Control. *Appl. Energy* **2015**, *149*, 104−116.
(32) DeSantis, D.; Mason, J. A.; James, B. D.; Houchins, C.; Long, J. R.; Veenstra, M. Techno-Economic Analysis of Metal−Organic Frameworks for Hydrogen and Natural Gas Storage. *Energy Fuels* **2017**, *31* (2), 2024−2032.

DOI: 10.1021/acscentsci.7b00186
ACS Cent. Sci. 2017, 3, 668−672